



An automatic welding defect location algorithm based on deep learning

Lei Yang¹, Huaixin Wang¹, Benyan Huo, Fangyuan Li, Yanhong Liu *

School of Electrical Engineering, Zhengzhou University, China and with the Robot Perception and Control Engineering Laboratory, Henan Province, 450001, China



ARTICLE INFO

Keywords:

Welding defects
Defect location
X-ray images
Data augmentation
Semantic segmentation

ABSTRACT

Welding production has a pivotal role in the modern manufacturing industry. However, welding defects are frequently generated during the complex welding production process which will bring a certain effect to the welding quality. Therefore, the issue of welding defect detection has received considerable critical attention. However, traditional methods, based on handcrafted features or shallow-learning techniques could only detect welding defects under specific detection conditions or priori knowledge. In this paper, to serve the evaluation of the harmfulness of welding defects to different objects, based on the strong feature expression ability of deep learning, an automatic welding defect location method is proposed based on the improved U-net network from digital X-ray images which includes data augmentation and welding defect location. To acquire better location performance, the data augmentation is realized to enlarge the data set of welding defects to serve the network training. On the basis, a defect location method based on the improved U-net network is proposed to realize automatic and high-precision welding defect location. Experiments show that the proposed method could acquire the detection precision up to 88.4% on the public data set (GDXray Set) which shows a remarkable location performance compared with other related detection methods.

1. Introduction

Nowadays, welding production is essential for a wide range of production applications, such as aircraft, automobile and shipbuilding. To reduce the human labor and improve the production efficiency, robot welding has got the rapid development over these past decades, and it is also a typical representative of intelligent manufacturing. However, during the complex welding process, welding quality is determined by much factors, such as welding current, welding voltage, welding speed and nozzle height. Therefore, welding defects are frequently generated during the robotic welding. Welding quality detection is the key procedure in the intelligent welding robots. It not only affects the appearance of products, but also the structural strength and performance of products. More seriously, it will cause some potential safety dangers to the users of products [1–3]. Non-destructive defect detection is an effective method and main means to detect the internal quality of different products. For important precision casting parts, in order to evaluate the harmfulness of minor defects, it is necessary not only to identify the existence of defects, but also to detect the location of defects. Therefore, to evaluate its impact on mechanical properties and provide decision-making basis for repairing, welding defect detection and

location are increasingly recognised as a serious, worldwide public concern.

The sensor is the key tool for welding defect detection and location. At present, the common sensors on welding defect detection include arc audible sound [4–6], radiographs [7,8], magneto-optical sensors [9], vision sensors [10] and X-ray detection [11–13]. Like the vision detection, the past decade has seen the rapid development of X-ray non-destructive detection. Compared with other detection methods, the X-ray non-destructive detection has better performance and it could acquire the internal structure and defect information of different products, so it could better identify and locate the welding defects. A considerable amount of literatures have been published on the defect detection from X-ray images. Duan et al. proposed a cascade AdaBoost algorithm to detect the welding defects from X-ray images [14], and it could well distinguish defects from non-defects. Zou et al. proposed a welding defect detection method based on Kalman filtering [15]. Jian et al. applied the X-ray detection to mobile phone screen glass. And he proposed a defect detection method based on machine vision [16]. Aimed at the food industry, Haff et al. proposed a defect detection method from the X-ray images [17]. To detect Ball Grid Array (BGA) package defects, Moore et al. propose a three-dimensional (3D) X-ray

* Corresponding author.

E-mail address: liuh@zzu.edu.cn (Y. Liu).

¹ L. Yang and H. Wang contribute equally to this work.

detection method, and experiments showed that it had better performance than 2D x-ray or other non-destructive methods [18]. In this paper, based on the good performance of the X-ray detection, it is adopted here for the detection task of welding defects.

At present, there have been a number of longitudinal studies involving in the defect detection. Chu et al. proposed a laser-based method to detect welding defect [19]. During this proposed method, a structured light sensor was designed to scan the whole weld beads. And the welding defect was done by the image processing of the laser stripe patterns. Li et al. also developed a welding defect detection method based on the structured light sensor [20]. The defect detection methods based on laser structured light have good robustness and high accuracy. However, the laser structured light belongs to local sensor, its measurement speed is slow and the measurement area is smaller. To realize fast defect detection, some image-based methods are proposed. In our previous work, a welding quality detection method based on shape from shading(SFS) was proposed [21]. To acquire the 3D profile of weld beads, the SFS algorithm was adopted to realize fast 3D reconstruction of weld beads. And the welding quality detection was done by the processing of 3D profile of weld beads. Malarvel et al. proposed an improved Otsu method for welding defect segmentation [22]. And it could automatically determine a desired threshold value for the defect segmentation. In the real welding production, industrial environment is always complex due to the much factors, such as weak texture, rust and spray paint. These factors will bring a certain effects to image processing and affect the robustness of the image-based methods.

With the fast development of machine learning and pattern recognition, a considerable literature has grown up around the combination of machine learning algorithm and welding robots to enhance the intelligence of welding robots, such as artificial neural network (ANN) [23], support vector machine (SVM) [24], k-nearest neighbor (KNN) [25]. Huang et al. proposed an improved SVM method to estimate different defects [26]. To get the best classification performance, the optimal parameters of SVM model were optimized by genetic algorithm (GA). Boaretto et al. proposed an improved multi-layer perceptron (MLP) to realize automatic detection of welding defects [27]. The back-propagation (BP) learning algorithm was combined with the MLP model to get better detection performance. Experiments showed that the proposed method on the test data could reach an accuracy of 88.6%. Das et al. proposed a defect detection method of friction stir welding based on support vector regression (SVR) model [28]. Experiments showed that the proposed method could get better results than ANN model and general regression model. Sambath et al. proposed a defect detection method based on ANN model [29]. It could obtain a classification rate up to 94%. Much experiments has proved the good detection performance of machine learning algorithm on welding defect detection. However, the machine learning algorithms rely on the artificially designed feature vector. How to design an effective image feature for the classification model still is a challenging work against complex welding environment and background.

Due to the improvement of big data and computing power, deep neural network (DNN) model has got great development [30]. It could process the original image data directly, and automatically discover and extract high-level image features through network training [31]. Compared with the conventional machine learning algorithm, it could avoid artificially designed feature vector and automatically realize some detection or recognition tasks. Nowadays, it has been applied much research fields, such as face detection [32], games [33] and autonomous vehicles [34]. At present, a number of researchers have sought to the applications of DNN model on industrial inspection [35,36]. Hou et al. built a deep convolution neural network (DCNN) for classifying different weld flaws [37]. Experiments showed that it could achieve an accuracy of 97.2% which was higher than the traditional machine learning models. Combined with transfer learning, Suyama et al. proposed a welded joint detection method from radiographic images [38]. To realize automatically feature extraction of laser welding images,

Gunther et al. designed the deep auto-encoding neural network which could extract salient, low-dimensional image features from high-dimensional laser welding images [39]. And the actor-critic reinforcement learning was adopted to do penetration control. Lin et al. proposed a robust casting defect detection method [40]. During the proposed method, the intra-frame attention algorithm was used to determine the suspicious defect areas. And the DCNN model was designed to exclude the missed detection. To inspect the welding defects, Park et al. proposed a detection method based on convolution neural network(CNN) model [41]. The proposed method included two steps which were realized by two designed CNN models. One CNN model was used to determine the area of welding defect and another CNN model was used to inspect the welding defect. However, much work is aimed at welding defect recognition and too little work has been devoted to the location task of welding defects. For important precision parts, in order to evaluate the harmfulness of welding defects, the location of welding defects is the basis to evaluate its impact on mechanical properties and maintenance decision. Therefore, this study makes a major contribution to research on the welding defect location combined with the advanced deep learning models.

According to the above analysis, to overcome these issues on welding defect detection, an automatic welding defect location method from digital X-ray images is proposed based on the improved U-net network. And it is verified on the public data set of X-ray welding images. The main contributions of this paper can be summarized as follows: (1).To keep better location performance, combined with image processing and image crop, an effective data augmentation method is proposed to enlarge the data sets and serve the network training. (2).An improved U-net network is proposed to realize automatic and high-precision welding defect location. (3).Compared with other advance detection models, the proposed method could well realize the high-precision location of welding defects without any prior knowledge and predetermined parameters.

The overall structure of this paper takes the form of five sections, including the introduction section. The remaining part of this paper is organized as follows: Section 2 is about the system framework of this paper. Section 3 describes the methods of data augmentation. Section 4 describes the proposed welding defect location method based on the improved U-net network. Section 5 is about the experiment results and discussion. Finally, the conclusions and prospects of this paper are described.

2. System framework

2.1. System configuration

To evaluate of the harmfulness of welding defects to different objects, such as structural strength and comprehensive quality, based on the good detection performance of X-ray detection [42–44], a welding defect inspection scheme is set up in this paper to acquire the internal defect structure of welding work pieces, as shown in Fig. 1.

For the X-ray welding images, the raw images have the unique characteristics which will bring a certain challenge to the high-precision location of the welding defects.

- (1). The X-ray welding images always present the weak-contrast and weak-texture features. It causes that the details about the welding defects are not prominent in the raw images.
- (2). The welding defects belong to the small pixel clustering or small edge. For the raw images of 4k length, how to realize the accurate defect detection on multi-scale objects still faces a certain challenge.

To address the above issues, to ensure the detection performance of the proposed method, some key links are needed to realize the automatic location of welding defects:

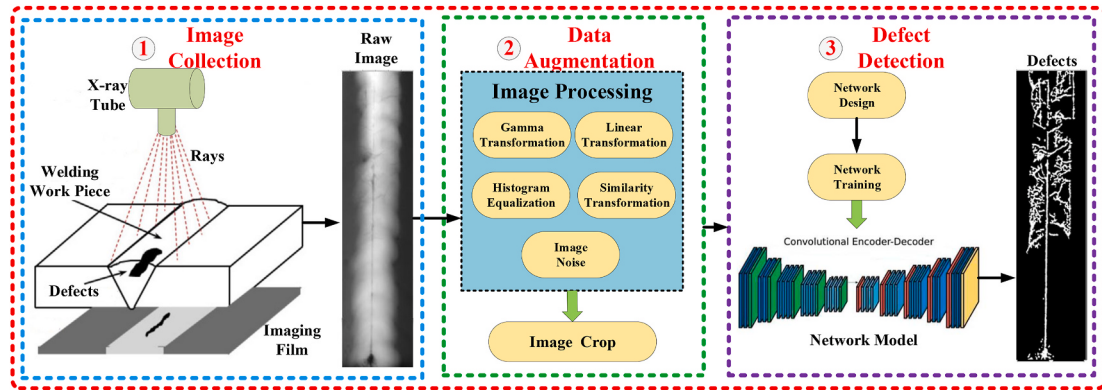


Fig. 1. The framework of the proposed method.

- (1). **Image collection:** To better realize the defect detection of welding work pieces, a good labeled data set is the premise for the proposed location model of welding defects.
- (2). **Data Augmentation:** The samples of X-ray welding images belong to the small-scale data set, the data augmentation needs to be done to enlarge the data set and serve the model training of deep detection model of welding defects.
- (3). **Defect Location:** Faced with the complex X-ray welding images with weak texture and weak contrast, an effective detection model is the core part for the automatic and high-precision location of welding defects.

2.2. Data set

Based on the inspection scheme in Fig. 1, a public experimental data set of X-ray detection is constructed for research and educational purposes only (**GDXray set** [45]). This public X-ray data set includes a subset about X-ray welding images (**Welds**) which is collected by the BAM Federal Institute for Materials Research and Testing, Berlin, Germany.

The **Welds** subset includes not only 10 X-ray images with 4k length and variable width (series W0001), but also the annotations of bounding boxes and the binary images of the ground truth of welding defects (series W0002). Meanwhile, to better serve the network training, series W0003 of **Welds** has more than 60 X-ray images and part of them is labeled in the form of the binary images with the help of experts engaged in robot welding. Some sample images of X-ray welding images from **Welds** set are shown in Fig. 2.

3. Data augmentation

The **GDXray set** just provides 10 X-ray welding images with labeled welding defects which could not meet the training requirements of deep neural networks. Due to the limitation of technical conditions, it is not easily to collect much X-ray welding images. And the pixel-level image annotation is a time-consuming and hard work. Meanwhile, the accurate image annotation about welding defects also rely on expert experience in welding field. Therefore, to get better detection performance of the proposed method, an effective data augmentation method is needed to enlarge the data set.

3.1. Image preprocessing

Machine vision provides a mature data processing method which could well process the raw images to generate some new images. It includes much effective image processing tools for data augmentation of small-scale samples, such as similarity transformation, gamma transformation (Eq. (1)), linear transformation (Eq. (2)), histogram equalization, image noise, etc, as shown in Fig. 1.

$$g = cr^\gamma \quad (1)$$

$$l = kr + b \quad (2)$$

Where g and l are the gray values after image transformation, r is the gray value of raw images. c and γ are the coefficients of gamma transformation. k and b are the coefficients of linear transformation.

Faced with the dark X-ray welding images in **GDXray set**, these tools could well process the raw images to generate some new images. And the

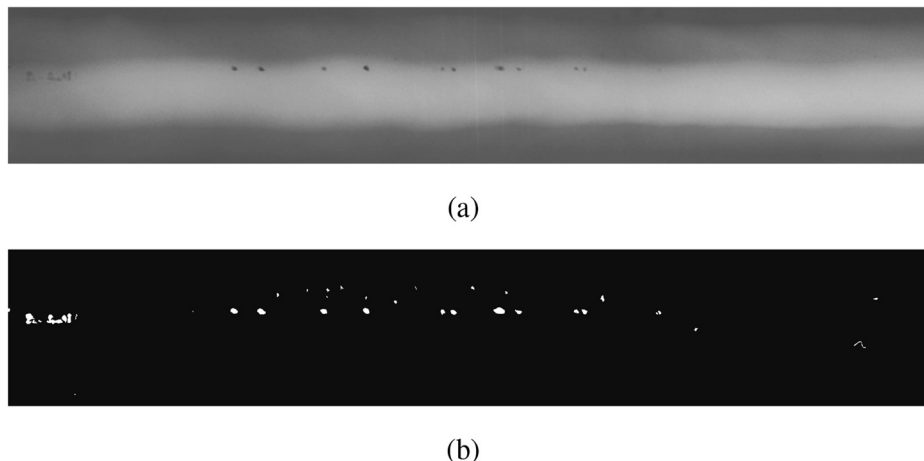


Fig. 2. Raw welding images.(a)The raw X-ray image; (b)The welding defect.

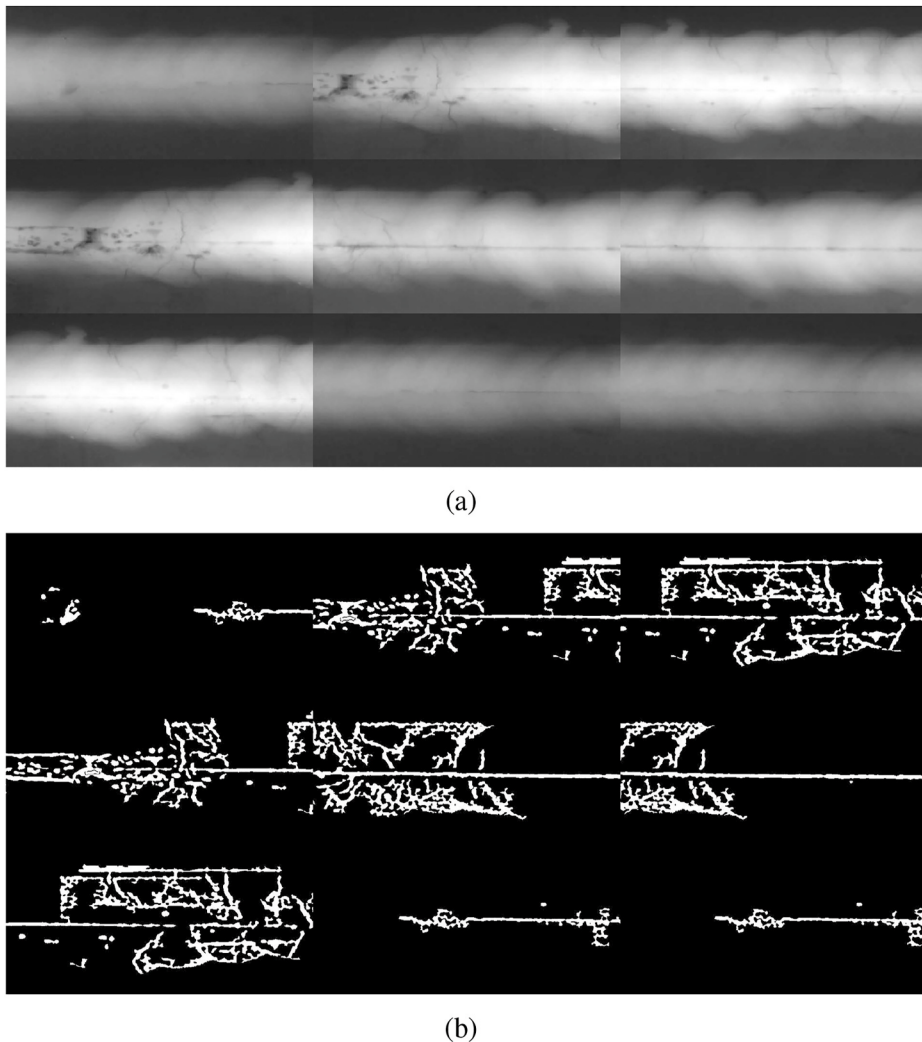


Fig. 3. Some cropped image patches of raw images. (a)Raw X-ray image patches; (b)Welding defect patches.

detailed parameters about image processing are shown in [Table 1](#).

On the basis, it is randomly divided into training and test sets by a 80:20 ratio. For the model evaluation, the training and test sets are disjoint and the test set does not include any augmented images.

3.2. Image crop

Although the image preprocessing could enlarge the data set to some extent, the data set still could not meet the training demands of deep neural network. Due to the raw welding images of 4k length, to produce more images, the random crop is adopted in the training set to process the raw images and enlarge the data set. For the test set, it is processed by uniform image crop for model evaluation. And image crop is also performed identically on the ground truth to ensure the image matching between the raw images and ground truth, as shown in [Fig. 3](#).

Fusion with the image processing and random crop, the experimental

Table 1
Parameter setting of image processing.

Index	Methods	Parameter Values
1	Similarity Transformation	Image Rotation (Angle = 180°)
2	Gamma Transformation	$c = 1, \gamma = 0.7$
3	Linear Transformation	$k = 0.85, b = 0.3$
4	Gaussian Noise	Means = 0, Covariances = 0.02
5	Histogram Equalization	-

Table 2
The results of data augmentation.

Index	Name	Values
1	Training Images	16
2	Test Images	4
3	Image Size	320*3840
4	Image Patch	320*640

Table 3
The values of network parameters.

Index	Name	Values
1	Input Image Size	320*640
2	Training Epoches	40000
3	Learning Rate	10^{-4}
4	Batch Size	8

results of data augmentation about X-ray welding images are shown as [Table 2](#).

4. Welding defect location

On the basis of data augmentation, an automatic location method about welding defects is proposed to provide an end-to-end detection

scheme to locate the welding defects and evaluate the harmfulness of welding defects (see Fig. 3).

4.1. Network structure

U-net network is a typical 2D full convolutional neural network which shows a good segmentation performance on the medical images, such as fMRI images and CT images [46]. Inspired by the U-net network, to enhance the segmentation performance on the X-ray welding images, an improved U-net network is proposed for high-precision defect segmentation. Fig. 4 shows the special network structure of the improved U-net network.

As shown in Fig. 4, the improved U-net network receives the gray X-ray welding images as the network input and generate the binary segmentation images with the same size as the network output. It is a typical U-type network structure which is composed by the Encoder and Decoder structures. They correspond to the left side and right side of the image respectively, as shown in Fig. 4.

(1). Encoder Network

The encoder network is used to reduce image feature size and its architecture is a repetitive structure with convolution layers and one max-pooling layer in each repetition. The encoder network begins with the convolutional (Conv) layer to realize the image down-sampling. It is followed by the batch normalization (BN), rectified linear unit (Relu) and max pooling layer. The max-pooling layer is inserted between two encoding layers. The BN is used to stabilize training, speed up the network convergence, and regularize the model. The ReLU activation function is shown as Eq. (3). The max-pooling layer is a 2x2 max pooling operation with stride 2 for feature down-sampling which could preserve the meaningful features with high activation, and eliminate some

unnecessary features. During each down-sampling, the channels of feature is doubled.

$$f(x) = \max(0, x) \quad (3)$$

(2). Decoder Network

Conversely, the decoder network is used to restore the spatial information and feature size. It is basically symmetrical to the encoder network and each decoding layer has a corresponding encoding layer in the decoder network. The up-sampling operation is used to reduce feature channels and enlarge feature maps from the encoder layer. Like the max pooling layer, the up-sampling layer is also inserted between two decoding layers.

(3). Skip Connections

For the encoder network, lower network layer could acquire the low-level feature maps with higher spatial resolution which are suitable for the small-scale defects. And more abstract and high-level feature maps could be acquired with the increase of the network layer which are very suitable for the large-scale defects.

To enhance the performance of the segmentation network on multi-scale welding defects, skip connections are added between the encoder and decoder network layers, as shown in Fig. 4. The purple connecting lines indicate the skip connections of U-net network, but it still fails in some small defects through experiment tests.

To improve the detection precision, on the basis of U-net network, an improved U-net network is proposed for defect segmentation and more skip connections are added into the segmentation network to circumvent the bottleneck of the information. As shown in Fig. 4, the red connecting lines indicate the new added skip connections.

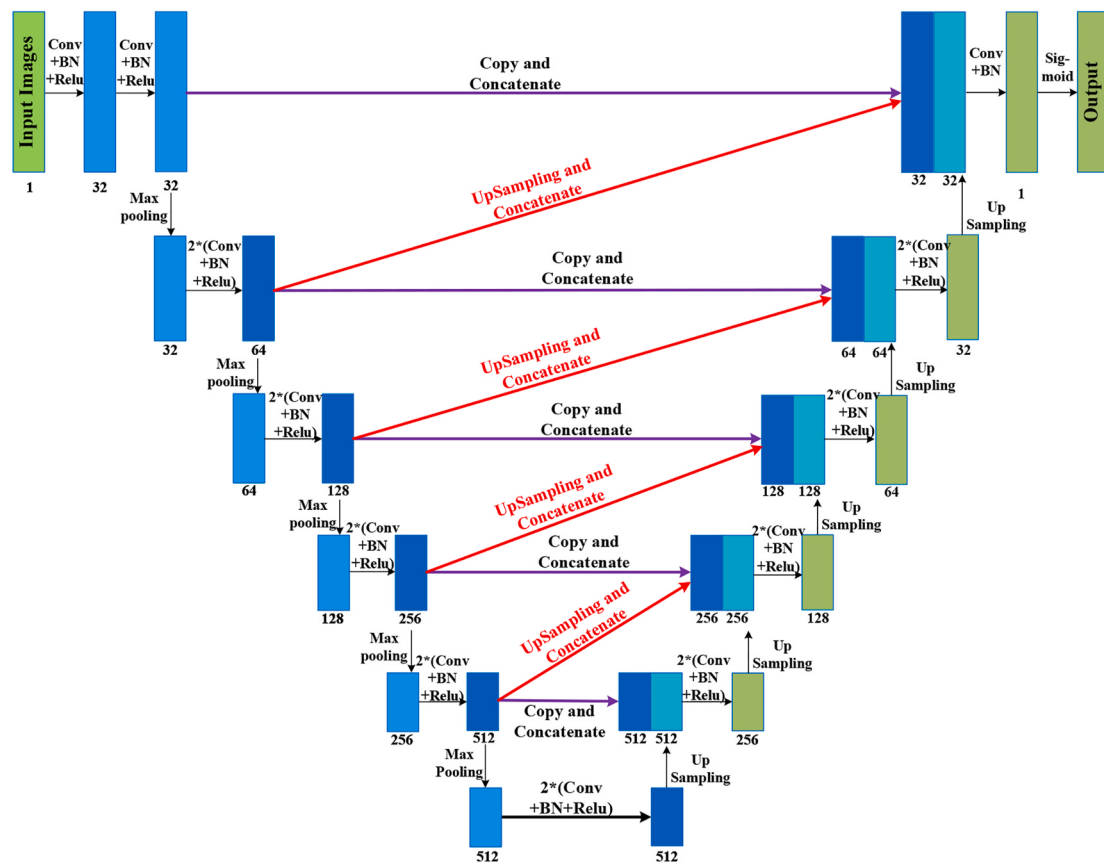


Fig. 4. The special network structure of the proposed network.

4.2. Loss function

An effective loss function is also a key part for the segmentation network which is used to indicate the training process and ensure the fast network convergence. Based on the good performance of the binary cross-entropy loss function, it is adopted as the loss function of the improved U-net network. The special definition of the objective loss function is shown as Eq. (4).

$$L_{\text{oss}} = - \sum t_i \log \hat{p}_i - (1 - t_i) \log (1 - \hat{p}_i) \quad (4)$$

Where t_i and \hat{p}_i denote separately the ground truth and prediction value.

5. Experiments and discussion

Through the detailed experiment analysis and comparison, the detection performance of the proposed method on the X-ray welding images is tested and discussed in this section. Meanwhile, to speed up the training and test processes of deep network model, the related experiments are performed on the NVIDIA GeForce RTX2080 Ti Card.

Firstly, the related evaluation indicators are introduced in this paper for the model evaluation. Secondly, the detection performance of the proposed method is verified based on the data set after data augmentation. Finally, some related advanced detection methods are introduced and set as comparison methods to show the effectiveness of the proposed method.

5.1. Evaluation indicators

To better verify the performance of proposed network model, some evaluation indicators are introduced here to verify the location results of welding defects.

1 .Precision-Recall (P-R) Curve: Precision(P) and Recall(R) are two important indicators of artificial intelligence to evaluate the neural network models, as shown in Eq. (5) and Eq. (6). And the P-R curve could be constructed by the organization of the P and R in two-dimensional space.

$$P = \frac{T_p}{T_p + F_p} \quad (5)$$

$$R = S_e = \frac{T_p}{T_p + F_n} \quad (6)$$

Where T_p and T_n denote true positive and true negative. F_p and F_n denote false positive and false negative.

2 .Sensitivity (S_e): Sensitivity is used to measure the proportion of positive pixels that are correctly identified, as Eq. (6).

3 .Specificity (S_p): Like the sensitivity, specificity is a similar indicator to measure the proportion of negative pixels that are correctly identified, as Eq. (7).

$$S_p = \frac{T_n}{T_n + F_p} \quad (7)$$

4 .Accuracy (A_{cc}): It is used to measure the proportion of all the pixels that are correctly identified, as Eq. (8).

$$A_{cc} = \frac{T_n + T_p}{T_p + T_n + F_p + F_n} \quad (8)$$

5 .Area under Curve (AUC): The value of AUC represents the area under the curve, such as P-R Curve, which is between 0.1 and 1. It could evaluate the performance of network intuitively. The bigger the AUC value, the better the model performance.

6 .Dice Coefficient (Dice): It is a similarity evaluation indicator between the prediction value and ground truth, as Eq. (9).

$$d = \frac{2|A \cap B|}{|A| + |B|} \quad (9)$$

Where d denote the similarity score. A and B denote two evaluation objects.

5.2. Network verification

Faced with the proposed deep semantic segmentation network, some parameters need to be initialized for the network training, as shown in Table .3. For the network training, the training epoches and learning rate are respectively set as 40000 and 10^{-4} .

Through the model training, the loss curve about the proposed method is shown as Fig. 5. It could be seen that the loss curve is converged rapidly before 5000 steps. And the convergence speed slows down after 5000 steps and is essentially stopped.

To better show the detection performance of the proposed method, some typical semantic segmentation networks are set as comparison methods to show the network effectiveness, such as U-net network,² conditional Generative Adversarial network (cGAN) [47]. And the cGAN network is composed by two parts: Generator and Discriminator, as shown in Fig. 6. The Generator tries to produce fake data like the ground truth. The Discriminator is introduced into the segmentation network to enhance the segmentation performance of the Generator which is used to distinguish whether the data is fake or real. Based on the segmentation performance of U-net network, it is adopted as the Generator. The detailed structure of the Discriminator is shown as Table .4.

And these network models are verified on the public data set of GDXray set, Fig. 7 shows the P-R curves of these network models. It could be seen that the proposed network could acquire a higher detection precision than other two networks on the X-ray welding images.

Further, to specifically show the detection performance of different network models, based on the introduced evaluation indicators in Section.V-A, these evaluation indicators of different networks are computed and shown as Table .5. Meanwhile, some X-ray welding images are also set as experimental images to show the segmentation performance more intuitively, the special segmentation results of different X-ray welding images based on different network models are shown in Fig. 8.

Table 4
The network structure of Discriminator.

Index	Type	Filters	Size	Stride
1	Conv	5*5	32	1
2	Conv	4*4	32	2
3	Conv	4*4	64	2
4	Conv	4*4	64	2
5	Conv	4*4	128	2
6	Conv	4*4	128	2
7	Conv	4*4	256	2
8	Conv	4*4	512	1
9	Conv	4*4	512	1
10	Avgpool			
11	Connected			

² Cnn-in-welding: <https://github.com/malakar-soham/cnn-in-welding/>.

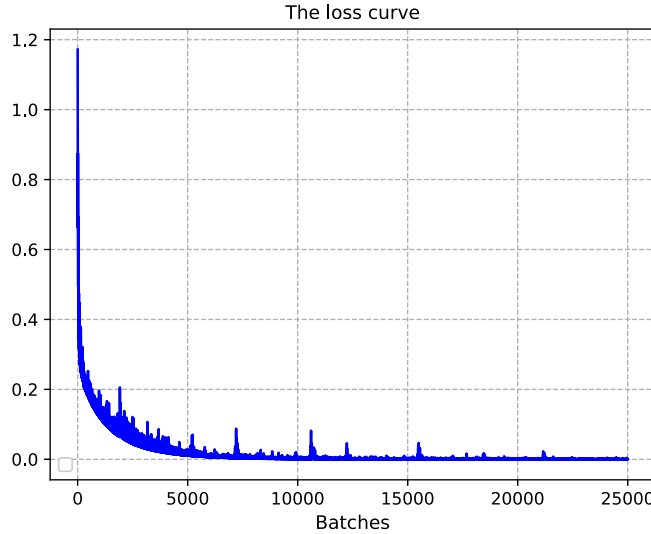


Fig. 5. The loss curve of the proposed method.

As shown in Fig. 8, the U-net network could solve the image segmentation issue to some extent. However, it fails in some samples due to the wrong segmentation results, such as Fig. 8 (a). Meanwhile, it has poor segmentation ability on the small segmentation noise compared with the proposed method.

And the cGAN network also acquires a worse segmentation results on the X-ray welding images due to much wrong segmentation results. It is mainly because the discriminator does not well indicate the training process which leads a poor segmentation performance of cGAN network compared with the U-net network.

On the contrary, based on more skip connections, through the feature fusion between different layers, the proposed method could well realize the multi-scale defect segmentation and the segmentation results include less noise. The segmentation performance has got greatly improved compared with these two network models.

Meanwhile, based on the above evaluation indicators in Table 5, due to relatively small pixel proportion of welding defects on the X-ray welding images, these segmentation networks could acquire the similar values on S_p and A_{cc} . And the proposed method acquires a similar S_e like U-net network. It is also critical to note that the proposed method could acquire higher values on the key evaluation indicators, such as AUC and D_{ice} . On the whole, the proposed network has higher segmentation precision on the X-ray welding images than other two networks.

Through the above experiment results and discussion, the proposed network shows an excellent detection performance on the data set of X-

ray welding images.

5.3. Performance comparison

Other than the typical semantic segmentation networks, some other related detection methods are also set as comparison methods to show the superiority of the proposed method, such as matched filter [48], stacking sparse auto-encoder (SSAE) network [35]. Based on the data set **GDXray set**, the detection results of different methods are shown in Fig. 9 and Fig. 10.

As shown in Fig. 9, the matched filter could realize the welding defect location on some samples, such as Fig. 9(b). However, it generates much wrong segmentation results, as shown in Fig. 9(a) and (d). The A_{cc} of matched filter on the X-ray welding images is 76.03% which is considerably lower than the mentioned network models in Section V-B. Therefore, the matched filter shows a poor detection performance on the X-ray welding images which could not meet the real detection demands of welding defects.

For the SSAE network, as shown in Fig. 10, it could realize the location of most welding defects from the X-ray welding images. However, it fails in some small welding defects. Meanwhile, for the mechanical property evaluation and maintenance decision, the visualization results are relatively poor which could not well indicate the internal defect structure of welding work pieces. Therefore, the proposed method has better performance on the location of welding

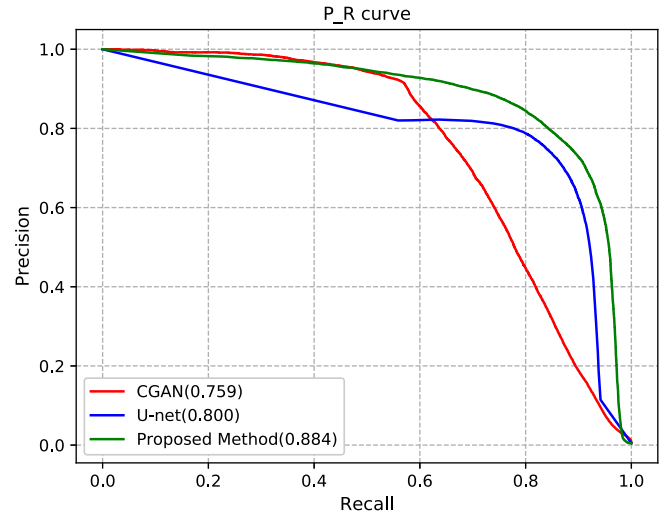


Fig. 7. The P-R curve of different models.

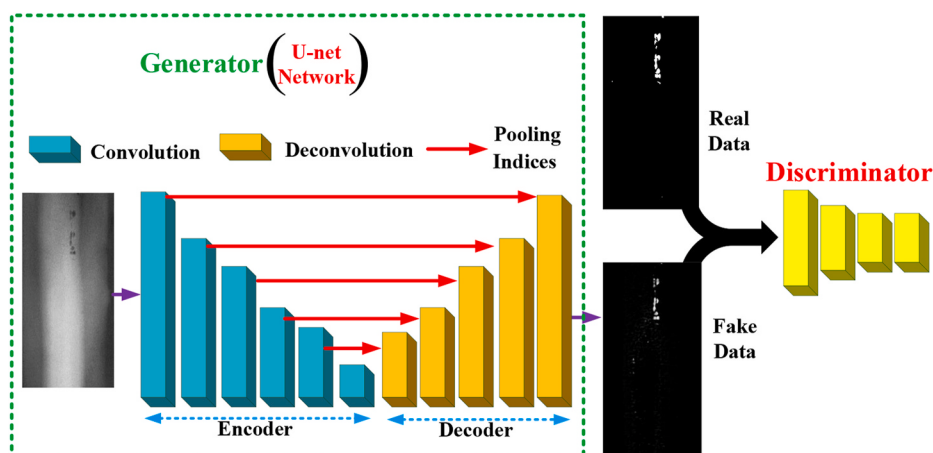


Fig. 6. The network structure of cGAN model [47].

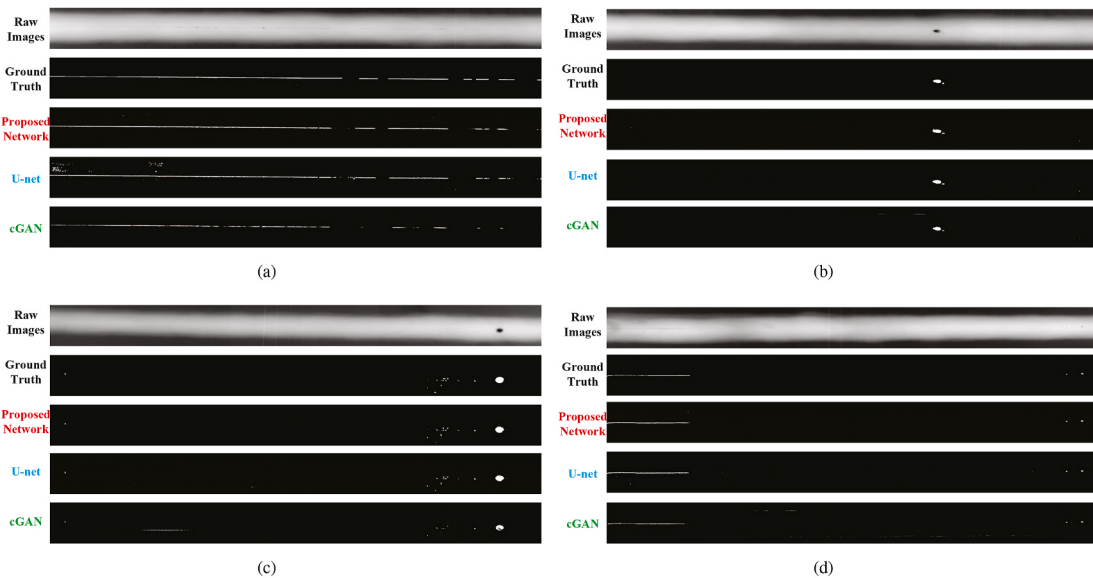


Fig. 8. Image segmentation of different X-ray welding images.

Table 5
The evaluation indicators of different networks.

Index	Name	U-net	cGAN	Proposed Network
1	S_e	0.864	0.618	0.860
2	S_p	0.998	0.999	0.999
3	A_{cc}	0.998	0.997	0.998
4	AUC	0.800	0.759	0.884
5	$Dice$	0.782	0.708	0.818

defects according to the above experimental analysis.

6. Conclusion

To serve the evaluation of the harmfulness of welding defects to different objects, an automatic location method of welding defects is proposed based on the improved U-net network from the digital X-ray

images. Based on the public data set-**GDXray set**, the proposed method could get a better detection performance on X-ray welding images, and it could realize the automatic and high-precision defect location without any prior knowledge and predetermined parameters. The main results of this paper are summarized as follows:

1. Faced with the small-scale samples of X-ray welding images, an effective data augmentation method is proposed combined with the image preprocessing and random crop to enlarge the data set and serve the model training of the deep semantic segmentation networks.
2. To realize automatic and high-precision location of welding defects, an improved U-net segmentation network is proposed to provide an end-to-end welding defect detection scheme from X-ray welding images.
3. Without any prior knowledge and predetermined parameters, the proposed method shows a better detection performance on the public data set compared with other related advanced detection algorithms.

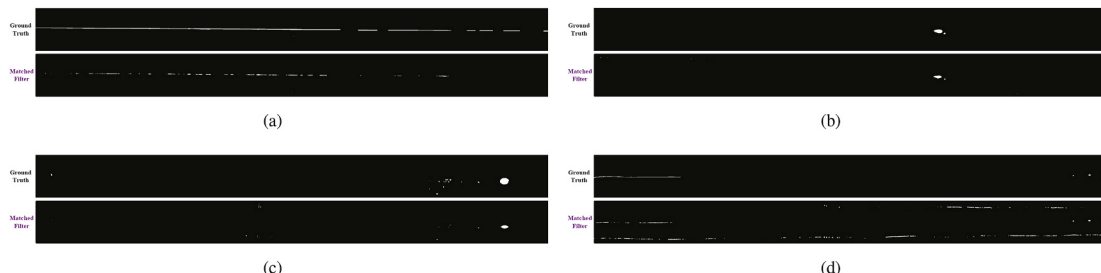


Fig. 9. Image segmentation of different X-ray welding images based on matched filter.

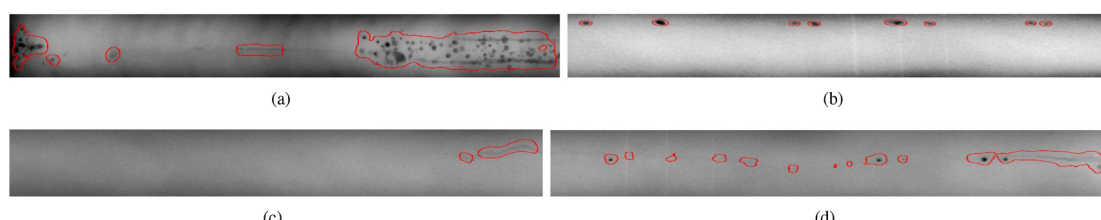


Fig. 10. The detection results based on SSAE [35].

In the future, we will continue this research work to improve the model performance, such as the location speed and precision of welding defects.

Author statement

No conflict of interest exists in the submission of this manuscript, and this manuscript is approved by all authors for publication. This work described was original research that has not been published previously, and not under consideration for publication elsewhere, in whole or in part.

We confirm that the manuscript has been read and approved by all named authors and that there are no other persons who satisfied the criteria for authorship but are not listed. We further confirm that the order of authors listed in the manuscript has been approved by all of us.

We confirm that we have given due consideration to the protection of intellectual property associated with this work and that there are no impediments to publication, including the timing of publication, with respect to intellectual property. We also confirm that we have followed the regulations of our institutions concerning intellectual property.

Funding

This work was supported by the National Key Research & Development Project of China (2020YFB1313701), the National Natural Science Foundation of China (No.62003309), Science & Technology Research Project in Henan Province of China (No.202102210098) and Outstanding Foreign Scientist Support Project in Henan Province of China (No. GZS2019008).

Declaration of competing interest

The authors declare that they have no known competing financial interests or personal relationships that could have appeared to influence the work reported in this paper.

Acknowledgment

The authors would like to thank the anonymous referees for their valuable suggestions and comments.

References

- [1] Sun J, Li C, Wu X, Palade V, Fang W. An effective method of weld defect detection and classification based on machine vision. *IEEE T Ind Inform* 2019;15(12): 6322–33.
- [2] Zhang Y, You D, Gao X, Zhang N, Gao PP. Welding defects detection based on deep learning with multiple optical sensors during disk laser welding of thick plates. *J Manuf Syst* 2019;51:87–94.
- [3] Ranjan R, Khan AR, Parikh C, Jain R, Mahto RP, Pal S, Pal SK, Chakravarty D. Classification and identification of surface defects in friction stir welding: an image processing approach. *J Manuf Process* 2016;22:237–53.
- [4] Zhang Z, Wen G, Chen S. Audible sound-based intelligent evaluation for aluminum alloy in robotic pulsed gtaw: mechanism, feature selection, and defect detection. *IEEE T Ind Inform* 2017;14(7):2973–83.
- [5] Yusof M, Kamaruzaman M, Zubair M, Ishak M. Detection of defects on weld bead through the wavelet analysis of the acquired arc sound signal. *J Mech Sci Technol* 2016;10(2):2031–42.
- [6] Lv N, Xu Y, Li S, Yu X, Chen S. Automated control of welding penetration based on audio sensing technology. *J Mater Process Technol* 2017;250:81–98.
- [7] Liao TW. Improving the accuracy of computer-aided radiographic weld inspection by feature selection. *NDT&E Int* 2009;42(4):229–39.
- [8] Nacereddine N, Goumeidane AB, Zion D. Unsupervised weld defect classification in radiographic images using multivariate generalized Gaussian mixture model with exact computation of mean and shape parameters. *Comput Ind* 2019;108:132–49.
- [9] Gao X, Ma N, Du L. Magneto-optical imaging characteristics of weld defects under alternating magnetic field excitation. *Optic Express* 2018;26(8):9972–83.
- [10] Naso D, Turchiano B, Pantaleo P. A fuzzy-logic based optical sensor for online weld defect-detection. *IEEE T Ind Inform* 2005;1(4):259–73.
- [11] Lin J, Ma N, Lei Y, Murakawa H. Measurement of residual stress in arc welded lap joints by cos α x-ray diffraction method. *J Mater Process Technol* 2017;243:387–94.
- [12] Roy RB, Ghosh A, Bhattacharyya S, Mahto RP, Kumari K, Pal SK, Pal S. Weld defect identification in friction stir welding through optimized wavelet transformation of signals and validation through x-ray micro-ct scan. *Int J Adv Manuf Technol* 2018; 99(1–4):623–33.
- [13] Malarvel M, Sethumadhavan G, Bhagi PCR, Kar S, Saravanan T, Krishnan A. Anisotropic diffusion based denoising on x-radiography images to detect weld defects. *Digit Signal Process* 2017;68:112–26.
- [14] Duan F, Yin S, Song P, Zhang W, Zhu C, Yokoi H. Automatic welding defect detection of x-ray images by using cascade adaboost with penalty term. *IEEE Access* 2019;7, 125 929–125 938.
- [15] Zou Y, Du D, Chang B, Ji L, Pan J. Automatic weld defect detection method based on kalman filtering for real-time radiographic inspection of spiral pipe. *NDT&E Int* 2015;72:1–9.
- [16] Jian C, Gao J, Ao Y. Automatic surface defect detection for mobile phone screen glass based on machine vision. *Appl Soft Comput* 2017;52:348–58.
- [17] Haff RP, Toyofuku N. X-ray detection of defects and contaminants in the food industry. *J Food Meas Charact* 2008;2(4):262–73.
- [18] Moore TD, Vanderstraeten D, Forsslund PM. Three-dimensional x-ray laminography as a tool for detection and characterization of bga package defects. *IEEE Trans Compon Packag Technol* 2002;25(2):224–9.
- [19] Chu H-H, Wang Z-Y. A vision-based system for post-welding quality measurement and defect detection. *Int J Adv Manuf Technol* 2016;86(9–12):3007–14.
- [20] Li Y, Li YF, Wang QL, Xu D, Tan M. Measurement and defect detection of the weld bead based on online vision inspection. *IEEE T Instrum Meas* 2009;59(7):1841–9.
- [21] Yang L, Li E, Long T, Fan J, Mao Y, Fang Z, Liang Z. A welding quality detection method for arc welding robot based on 3d reconstruction with sfs algorithm. *Int J Adv Manuf Technol* 2018;94(1–4):1209–20.
- [22] Malarvel M, Sethumadhavan G, Bhagi PCR, Kar S, Thangavel S. “An improved version of otsu’s method for segmentation of weld defects on x-radiography images. *Optik* 2017;142:109–18.
- [23] Shukur OB, Lee MH. Daily wind speed forecasting through hybrid kf-ann model based on arima. *Renew Energy* 2015;76:637–47.
- [24] Erfani SM, Rajasegarar S, Karunasekera S, Leckie C. High-dimensional and large-scale anomaly detection using a linear one-class svm with deep learning. *Pattern Recogn* 2016;58:121–34.
- [25] Zhang S, Li X, Zong M, Zhu X, Wang R. Efficient knn classification with different numbers of nearest neighbors. *IEEE T Neur Net Lear* 2017;29(5):1774–85.
- [26] Huang Y, Wu D, Zhang Z, Chen H, Chen S. Emd-based pulsed tig welding process porosity defect detection and defect diagnosis using ga-svm. *J Mater Process Technol* 2017;239:92–102.
- [27] Boaretto N, Centeno TM. Automated detection of welding defects in pipelines from radiographic images dwdi. *NDT&E Int* 2017;86:7–13.
- [28] Das B, Pal S, Bag S. Torque based defect detection and weld quality modelling in friction stir welding process. *J Manuf Process* 2017;27:8–17.
- [29] Sambath S, Nagaraj P, Selvakumar N. Automatic defect classification in ultrasonic ndt using artificial intelligence. *J Nondestr Eval* 2011;30(1):20–8.
- [30] Silver D, Huang A, Maddison CJ, Guez A, Sifre L, Van Den Driessche G, Schrittwieser J, Antonoglou I, Panneershelvam V, Lanctot M, et al. Mastering the game of go with deep neural networks and tree search. *Nature* 2016;529(7587): 484.
- [31] Chen G, Lu C, Huang G, Chen Z. Automatic recognition of weld defects in tofd d-scan images based on faster r-cnn. *J Test Eval* 2018;48(2).
- [32] Sun X, Wu P, Hoi SC. Face detection using deep learning: an improved faster r-cnn approach. *Neurocomputing* 2018;299:42–50.
- [33] Wu I-C, Lee C-S, Tian Y, Müller M. Guest editorial special issue on deep/reinforcement learning and games. *IEEE T Games* 2018;10(4):333–5.
- [34] Yang S, Wang W, Liu C, Deng W. Scene understanding in deep learning-based end-to-end controllers for autonomous vehicles. *IEEE T Syst Man Cy Syst* 2018;49(1): 53–63.
- [35] Hou W, Wei Y, Guo J, Jin Y, et al. Automatic detection of welding defects using deep neural network. *J phys: Conf ser* 2017;vol. 933:012006. 1. IOP Publishing.
- [36] Pan H, Pang Z, Wang Y, Wang Y, Chen L. A new image recognition and classification method combining transfer learning algorithm and mobilenet model for welding defects. *IEEE Access* 2020;8, 119 951–119 960.
- [37] Hou W, Wei Y, Jin Y, Zhu C. Deep features based on a dcnn model for classifying imbalanced weld flaw types. *Measurement* 2019;131:482–9.
- [38] Suyama FM, Delgado MR, da Silva RD, Centeno TM. Deep neural networks based approach for welded joint detection of oil pipelines in radiographic images with double wall double image exposure. *NDT & E Int* 2019;105:46–55.
- [39] Günther J, Pilarski PM, Helfrich G, Shen H, Diepol K. Intelligent laser welding through representation, prediction, and control learning: an architecture with deep neural networks and reinforcement learning. *Mechatronics* 2016;34:1–11.
- [40] Lin J, Yao Y, Ma L, Wang Y. Detection of a casting defect tracked by deep convolution neural network. *Int J Adv Manuf Technol* 2018;97(1–4):573–81.
- [41] Park J-K, An W-H, Kang D-J. Convolutional neural network based surface inspection system for non-patterned welding defects. *Int J Precis Eng Manuf* 2019; 20(3):363–74.
- [42] Wei Y, Liu X. “Dangerous goods detection based on transfer learning in x-ray images,” *Neural Computing and Applications*. 2019. p. 1–14.
- [43] Yang J, Zhao Z, Zhang H, Shi Y. Data augmentation for x-ray prohibited item images using generative adversarial networks. *IEEE Access* 2019;7, 28 894–28 902.
- [44] Riffó V, Godoy I, Mery D. Handgun detection in single-spectrum multiple x-ray views based on 3d object recognition. *J Nondestr Eval* 2019;38(3):1–11.
- [45] Mery D, Riffó V, Zschepel U, Mondragón G, Lillo I, Zuccar I, Lobel H, Carrasco M, Gdxray “. The database of x-ray images for nondestructive testing. *J Nondestr Eval* 2015;34(4):42.

- [46] Ronneberger O, Fischer P, Brox T. U-net: convolutional networks for biomedical image segmentation. In: International Conference on medical image Computing and computer-assisted intervention. Springer; 2015. p. 234–41.
- [47] Gao Z, Yang G, Li E, Shen T, Wang Z, Tian Y, Wang H, Liang Z. Insulator segmentation for power line inspection based on modified conditional generative adversarial network. Journal of Sensors 2019:1–8. 2019.
- [48] Elson J, Precilla J, Reshma P, Madhavaraja NS. Automated extraction and analysis of retinal blood vessels with multi scale matched filter. In: Proceedings of international conference on intelligent computing, instrumentation and control technologies. IEEE; 2017. p. 775–9.